U.P.B. Sci. Bull., Series C, Vol. 84, Iss. 3, 2022 ISSN 2286-3540

# UPGRADING A GPR SYSTEM TO CONDUCT LOW-ALTITUDE AERIAL GEOPHYSICAL INVESTIGATIONS

Iulian Alexandru CHELMUS[1], Cosmin Karl BANICA[2], Octavian Mihai GHITA[3]

*This article presents the modifications made to a GPR system in order to perform aerial geophysical investigations from low altitude. Such investigations used in archeology and not only, bring in addition to those performed on the ground many benefits, such as a higher speed of investigation, the possibility of measurements in hard-to-reach areas, a larger area covered during measurements, etc. After upgrading the GPR system, laboratory tests were performed to verify the proper functioning of the system and to eliminate possible errors.*

**Keywords**: aerial, GPR, archeology, UAV.

## 1. Introduction

The proposed equipment complements a complex unmanned aerial vehicle (UAV) with remote sensing capabilities (multispectral, thermal and high-resolution photo camera) [1] by adding a ground penetration radar (GPR) system. This sensor package, which leads to a new, broader type of documentation / investigation, ensures the ability to associate remote sensing data with GPR investigations. We emphasize that all investigations - remotely controlled, or scheduled - deliver real-time data for horizontal surfaces with a high accuracy of the order of centimeters and a maximum penetrability of about 2 meters, depending on the propagation environment and the altitude of the system.

Ground penetration radar (GPR) is a non-invasive prospecting technique that uses electromagnetic radiation. Its operating principle is based on the emission of electromagnetic waves in the microwave field, using frequencies between 30 MHz and 30 GHz, to the ground and recording of the reflected signal. By analyzing the flight time and the way the radiation propagates, it is possible to identify changes in stratigraphy and / or the presence of some artefacts.

It is a non-destructive method, fact that give it a major importance in conducting investigations and with a unanimous recognition of its advantages in

[1] Researcher, Dept. of Advanced methods and techniques for artwork restoration & conservation The National R& D Inst. for Optoelectronics, Romania, e-mail: alexandru.chelmus@inoe.ro
[2] Assoc. Prof., Dept. of Measurements, Electrical Devices and Static Converters, Univ. POLITEHNICA of Bucharest, Romania, e-mail: cosmin.banica@upb.ro
[3] Prof., Dept. of Measurements, Electrical Devices and Static Converters, Univ. POLITEHNICA of Bucharest, Romania, e-mail, octavian.ghita@upb.ro

archaeological prospecting, especially the fact that it can be used to identify objects regardless of their constituent nature. Although the technique was described in 1910, it was not until the mid-1970s that it was first used in archeology at Chaco Canyon in New Mexico [2]. GPR prospecting is used today mainly from the ground level in many areas of industry and research, such as archeology, architecture, civil engineering, geology, forensics, agriculture and special applications.

Fig. 1. GPR system

Reported applications on aerial GPR investigations are rare [3], [4] and the extension to urban archeology and civil engineering is still ongoing [5]. There are no final reports for high-resolution GPR aerial investigation systems in these areas. However, there is a noticeable need and desire worldwide for an increased speed of investigation, as well as for covering larger areas using the GPR method [6], the system presented in this article meeting these requirements.

Carrying out aerial GPR investigations from low altitude compared to those performed classically, from the ground, brings many novelty elements and major advantages [7]:

- Scheduled flights can be synchronized with other remote sensing data records using the same flight path that allows data to be correlated;
- The addition of a sensor capable of conducting low-altitude radar investigations will complete the existing package of sensors for aerial imaging investigations, thus obtaining not only information about the ground surface but also about the subsoil;
- The area covered during the GPR investigations in the air is larger than that of the investigations carried out on the ground;
- The possibility of researching difficult areas (rugged surfaces, at high altitudes, with high slopes, surrounded by water, areas with vegetation, etc.);
- Higher investigation speed than ground-coupled GPR (10 m/s for aerial investigation vs. 2 m/s for average human speed under optimal conditions) while eliminating the human physical exhaustion factor;
- The automatic scheduled flight provided by UAV capabilities allows stand-alone operation, night-time investigations and eliminates the human error factor.

In order to make the low-altitude aerial GPR investigation system functional, it is necessary to upgrade it using two subassemblies, one that allows the remote control of the operator over the GPR system (both for changing the parameters of real-time data acquisition, but also for data visualization) and a stabilized support subassembly that ensures the parallelism of the GPR antenna with the ground during the measurements while limiting the vibrations induced by the GPR system aspect that limits the measurement errors.

The improved drone-mounted GPR system is designed to access hard-to-reach areas using conventional solutions. Combining modern drone technology with the ground penetration radar system, the aim was to develop a tool that could map surfaces in areas with difficult or risky access.

## 2. Design and development of the real-time remote viewing and control subassembly for the GPR system and the stabilized support

### 2.1 GPR real-time visualization and control subassembly

In order to be able to perform GPR investigations from the air but also to ensure the quality of the acquired data, a subset of remote real-time visualization and control has been developed for the existing GPR system.

From a technical point of view, the frequency must be considered as the frequency of radio waves emitted by the GPR system for investigations, so the bidirectional connection cannot be used radio waves that would cause disturbances in the acquired data. The GPR antenna to be used for aerial GPR investigations has a central frequency of 800MHz.

In order to create the software that allows the ground control of the aerial GPR system, two important technical aspects must be taken into account:

-the first is the need for a two-way connection. Thus, the change in the parameters of the data acquisition by the user on the ground is transmitted to the control unit mounted on the drone, and the data acquired by the control unit on the drone are transmitted to the ground to give the user the ability to view the data in real time.

- the second is represented by the communication protocol between the two components as well as the technical specifications regarding the transfer speed, for this purpose the technical specifications of interest of the two components were briefly attached.

The integrated radar control unit is mounted directly on the shielded antenna and externally powered. The built-in electronic design makes it a lightweight, compact system that is easy to assemble and operate.


Fig. 2. GPR control unit

*Table 1*

**GPR control unit specifications**

| | |
|---|---|
| Pulse repeat frequency | 100 kHz (standard) |
| Data bits | 16 |
| Communication speed | > 700 kbps |
| Data transfer rate | 40-400 kB / s at 4Mbit / s |
| Operating time | > 10 hours with standard battery accessories |
| Power supply | 12V DC external battery |
| Operating Temperature | -20 ° C to + 50 ° C |
| Communication protocol | IEEE 1248 (ECP) |

Component 2, the GPR system monitor is a dedicated tool, optimized for collecting, manipulating, processing and presenting GPR data. The user interface has been designed to be simple, intuitive and easy to use. Its unique dual function button allows easy navigation. The monitor has been designed for field use; the robust housing is IP65 and has an impact resistant screen.

Fig. 3. GPR monitor

Considering the importance of perfect synchronization between the two radar components and the desire to minimize possible errors, another remote-control solution of the GPR system was implemented. The solution consists in mounting the two components on the drone and creating an assembly that allows live video transmission of data directly from the monitor to the ground operator as well as creating a remote-controlled actuator to facilitate operator control (change acquisition parameters, start / stop recording, etc.

In order to make it possible to view and control the real-time remote control for the GPR aerial system, two stages were completed. The first stage was the physical design of the system that was mounted on the GPR system monitor. This design stage was the starting point for the realization of the command-and-control software component because it defines the components that will be integrated in the system. The second stage consisted in the effective realization of the command-and-control software for the components included in the system as well as the real-time data transmission.

The developed system is a system of translating an analog control method into a remote-control method. The system translates the user's interaction and transmits it remotely for analog system control, an interaction monitored via a high-quality video stream that can be viewed on a tablet, laptop or phone. The chosen approach is easy to implement due to the customized construction of the chassis and the command-and-control components and facilitates the interaction with the analog equipment located at a distance.

*Table 2*

**Results of the first stage: Physical design of the system**

| | |
|---|---|
| Decomposed view of the system |  |
| Assembly of components, assembly version | 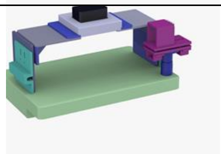 |
| Assembly of components plus analog module fixing system | 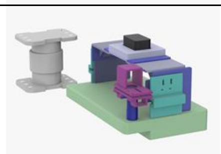 |
| The final system mounted on the GPR monitor | 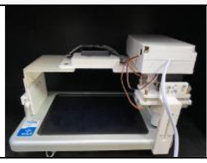 |

The following is the software for modifying the acquisition parameters and real-time data visualization for the GPR system:

```
// PINI
// ============================================
==========
// PIN RADIO RECEIVER
// --------------------
#DEFINE PIN_VT 8
#DEFINE PIN_DATA0 9
#DEFINE PIN_DATA1 10
#DEFINE PIN_DATA2 11
#DEFINE PIN_DATA3 12
#DEFINE PIN_ENABLE 13

// SERVOMOTOR PINS
// --------------------
#DEFINE PIN_SERVO_BTN 2
#DEFINE PIN_SERVO_POT 3

// REMOTE CONTROL BUTTON CODES
// ========================================
==================
#DEFINE RM_BTN_A 2
#DEFINE RM_BTN_B 8
```

```
#DEFINE RM_BTN_C 1
#DEFINE RM_BTN_D 4

//
%%%%%%%%%%%%%%%%%%%%%%%%%%%%
%%%%%%%%%%%%%%%%%%%%!%%%%%%%%
%%%%%%%%%%%%%%%%%%%%
// MOVE PARAMETERS SERVO BUTTON PANEL
//
%%%%%%%%%%%%%%%%%%%%%%%%%%%%
%%%%%%%%%%%%%%%%%%!
%%%%%%%%%%
%%%%%%%%%%%%%%%%%%%
#DEFINE RELAXATION_ANGLE_BTN 60.0 // [GRADE]
#DEFINE PRESS_ANGLE_BTN 20.0 // [GRADE]
#DEFINE PRESSURE_DURATION 400 // [MS] ONLY IF
NEEDED

// %%%%%%%%%%%%%%%%%%%%
%%%%%%%%%%%%%%%%%%%!
%%%%%%%%%%%%%%%%%%%%%%%%%%%
// MOTION PARAMETERS SERVO POTENTIOMETER
PANEL
// %%%%%%%%%%%%%%%
%%%%%%%%%%%%%%%%%!
%%%%%%%%%%%%%%%%%%%%%%%%%%%
#DEFINE SPEED_PERCENTAGE 10 // [%] POSITIVE VALUE,
BETWEEN 0 AND 100%

// DEFAULT PARAMETERS LIBRARY SERVO
// CAUTION FOR CONTINUOUSLY ROTATING SERVO,
THE WRITE () FUNCTION PARAMETER IS NOT
// ANGLE, THERE SPEED!
// DESCRIPTION OF THE WRITE () FUNCTION HERE:
// HTTPS://WWW.ARDUINO.CC/EN/REFERENCE/
SERVOWRITE
#DEFINE SPEED_MAX_SENS_ORAR 0
#DEFINE SPEED_MAX_SENS_ANTIORAR 180
#DEFINE SERVO_STOP 90

// CALCULATED VALUES
#DEFINE SPEED_TIME_TIME (INT) (SERVO_STOP * (1 -
PROCENT_ SPEED / 100.0))
#DEFINE SPEED_SLIFT_IN (INT) (SERVO_STOP +
(SPEED_MAX_SENS_PROVEL - SERVO_STOP) * \
PERCENTAGE SPEED / 100.0)

// OBJECT DEFINITIONS IN THE APPLICATION
// ============================================
========================
// RADIO REMOTE CONTROL OBJECT
RM4 REMOTE (PIN_DATA0, PIN_DATA1, PIN_DATA2,
PIN_DATA3);

// BUTTON SERVOMOTOR (TWO SERVOS ON THE SAME
COMMAND)
SERVICE SERVOBTN;
// SERVOMOTOR POTENTIOMETER
SERVICE SERVOPOT;

VOID SETUP () {
// INIT SERIAL COMM
SERIAL.BEGIN (9600);

// SETUP SERVO
// ==========================================
========================
SERVOBTN.ATTACH (PIN_SERVO_BTN);
SERVOPOT.ATTACH (PIN_SERVO_POT);

// PUT THE SERVO BUTTON IN THE FREE POSITION
SERVOBTN.WRITE (UNGHI_RELAXARE_BTN);

// STOP SERVO POTENTIOMETER
SERVOPOT.WRITE (SERVO_STOP);

// SETUP REMOTE CONTROL RECEIVER
// ========================================
========================
// CONFIG BTN C, B, D, AS INPUT
// PINMODE (RM_BTN_C, INPUT_PULLUP);
// PINMODE (RM_BTN_B, INPUT_PULLUP);
// PINMODE (RM_BTN_D, INPUT_PULLUP);
PINMODE (RM_BTN_C, INPUT);
PINMODE (RM_BTN_B, INPUT);
PINMODE (RM_BTN_D, INPUT);

// CONFIG VT AS INPUT
PINMODE (PIN_VT, INPUT);

// TURN ON THE HANDSET
PINMODE (PIN_ENABLE, OUTPUT);
DIGITALWRITE (PIN_ENABLE, HIGH);

// SAY YOU SETUP
SERIAL.PRINTLN ("SETUP DONE");
}

VOID LOOP () {
CHAR VTPIN;

// READ THE CODE OF THE REMOTE CONTROL BUTTON
CONST INT BTNCODE = REMOTE.BUTTONCODE ();

// READ THE STATUS OF THE "VALID TRANSMISSION"
(VT) PIN
VTPIN = DIGITALREAD (PIN_VT);

// IF THE TRANSMISSION IS VALID
// IF (VTPIN! = 0) {
// SERIAL.PRINT ("BTNCODE =");
// SERIAL.PRINTLN (BTNCODE);

// DISPATCHER AND ORDER EXECUTION
// ============================================
===============
SWITCH (BTNCODE) {
// CODE FOR PANEL BUTTON - REMOTE CONTROL
BUTTON "C"
CASE RM_BTN_C:
// PRESS THE BUTTON
SERVOBTN.WRITE (PRESS_ANGLE _BTN);
// HOLD ON
DELAY (PRESSURE_DURATION);
// RELEASE THE BUTTON
SERVOBTN.WRITE (RELAXATION_ANGLE _BTN);
BREAK;
CASE RM_BTN_B:
// CODE FOR POTENTIOMETER: ASCENDING DIRECTION
 REMOTE CONTROL BUTTON "B"
// ROTATE CONTINUOUSLY CLOCKWISE, WITH THE
SPECIFIED SPEED
SERVOPOT.WRITE (SPEED_TIME_WATCH);
BREAK;
CASE RM_BTN_D:
// CODE FOR POTENTIOMETER: DESCENDING
DIRECTION REMOTE CONTROL BUTTON "D"
// TURNS CONTINUOUSLY COUNTERCLOCKWISE,
WITH
THE SPECIFIED SPEED
SERVOPOT.WRITE;
BREAK;
// UNUSED - REMOTE CONTROL "A" BUTTON
CASE RM_BTN_A:
BREAK;
DEFAULT:
// STOP THE POWER SUPPLY
SERVOPOT.WRITE (SERVO_STOP);
BREAK;
}
//}
}
```

The software presented above was written on an Arduino that allows the translation and transmission of user commands to the 360 ° continuous rotation servomotor. This servomotor allows bidirectional rotation, and the pulse duration determines the speed and direction of rotation. The characteristics for which this servomotor was chosen are 5.5 kg/ m and a speed of 0.22 sec/60 ° ≈ 45 rpm, both being obtained at a voltage of 4.8V. Other electrical components of the command-and-control subassembly are the SG90 servomotor and the XL4015 descending DC-DC source. The SG90 servo motor has a high mechanical power and can rotate approximately 180 degrees (90 in each direction). It was chosen because a controlled angle rotation was desired without building a motor controller with feedback and gearbox, a limitation imposed by the limited space allocated to this subassembly.

The user can control the GPR system by using a 4-channel / 4-button remote control compatible with Arduino that has a telescopic antenna that ensures a working distance in direct visibility of up to 300m.

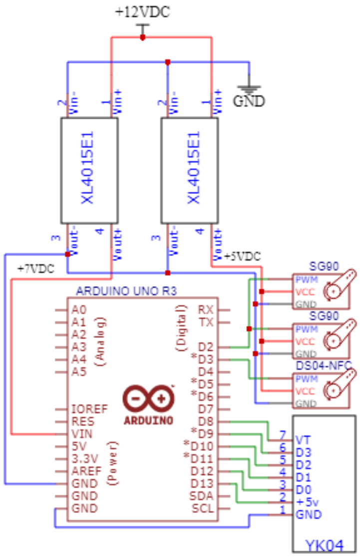


Fig. 4. Wiring diagram of the remote control subassembly

## 2.2 Stabilized support subassembly for the GPR system

For mounting the GPR antenna and the control unit on the unmanned aerial system it was also necessary to create a 3D gyro-stabilization system with the role of stabilizing the antenna during data acquisition to minimize errors. It was mounted on the existing mounting devices on the bottom of the drone specially designed for mounting sensors.

The design of the 3D gyro-stabilization system for the radar antenna is composed of:

- Gimbal mounting plate on the drone. An additional battery can be mounted on this mounting plate to power the system;

- 2 stepper motors controlled by a microcontroller, through which the antenna is permanently positioned parallel to the ground. With this microcontroller you can control the positioning of the antenna from another angle.
- Carbon fiber frame on which are mounted the two motors used in gyro stabilization.
- Microcontroller consisting of control board, 2 accelerometers, 2 encoders, software command and control.
- Power supply between 12v-24v.

When constructing the stabilized support, the operating principle of the radar and its sensitivity to the presence of the electromagnetic field were taken into account. For these reasons, the material chosen to create the support is glass-textured with a thickness of 2 mm. Although carbon is generally used for drones and sensor mounts, due to its rigidity and low weight, in this case there was a fear that it would shield some of the radiation emitted by the antenna. In order to eliminate the possible electromagnetic field produced by the stabilization motors, servomechanisms were used at a voltage of 5V and controlled in PWM. Two servomotors were installed: 1 for the river axis and one for the pitch axis. The engines used generate 3kgf and act on the gimbal assembly by means of a lever. An autopilot equipped with a gyroscope, accelerometer, barometer and GPS was used for navigation and stabilization. It has the possibility to control through the stabilization algorithm (with a stabilization law of PID type), the servomotors, so that the radar antenna remains permanently horizontal. The tilt angle can be between 0 and 45 °. The location is done through the GPS interface. Data transmission is done by telemetry, using the MavLink protocol. The data reception is done through the Mission Planer software interface, in which the evolution of the equipment can be followed in real time, within a radius of approximately 1km.

*Table 3*

**Stabilized support for GPR system mounting on UAV**

| | |
|---|---|
| Design side view | 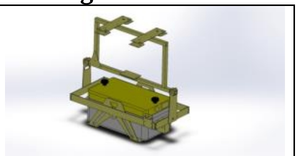 |
| Stabilized support built on the project |  |

| | |
|---|---|
| Stabilized support for mounting GPR system on UAV in final form |  |

## 3. Laboratory tests of the upgraded GPR system to perform low altitude aerial geophysical investigations

The activity that followed the construction of the components and the writing of the code needed to perform aerial GPR investigations was testing. The tests were performed in the laboratory and aimed at the proper functioning of the system.

The first test performed consisted of a comparative analysis of GPR data purchased with and without the remote control and visualization subassembly. In this sense, two radar measurements were performed in the laboratory using the 800MHz antenna that is used in aerial investigations. The measurements were made using the same parameters and with the antenna in the same position, the only difference being that the first measurement was performed directly by the user and the second through the real-time remote-control software. The table below shows the two measurements obtained.

*Table 4*

**Comparative analysis of GPR data**

| | |
|---|---|
| Measurements performed by direct user interaction with the GPR system | 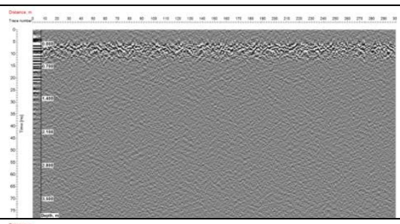 |
| Measurements performed using real-time remote-control software | 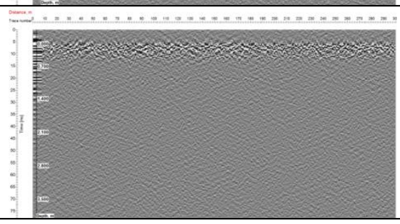 |

The tests showed that the use of the software did not induce changes in the acquired data; there was no interference or signal loss. Two more test scenarios and experimental analysis were developed in a complete configuration of the system, these aimed at observing the proper functioning and validation in order to conduct in situ investigations. The first test scenario aims to verify the influence of the stabilized support on the GPR data. The second scenario aims to verify the influence of the electromagnetic field produced by the drone motors on the GPR antenna.

The first test scenario was reproduced in the laboratory and was performed after mounting the 800 MHz GPR antenna in the stabilized support. The measurements were made using the same parameters and with the antenna in the same position, the only difference was the power supply to the motors of the servomechanisms of the stabilized support.

*Table 5*

**Check for interference produced by the motors of the servomechanisms of the stabilized support**

| | |
|---|---|
| Test with the engines of the stabilization servomechanisms stopped | 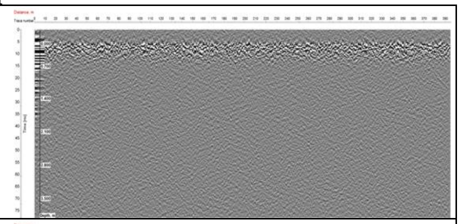 |
| Test with the engines of the stabilization servomechanisms running | 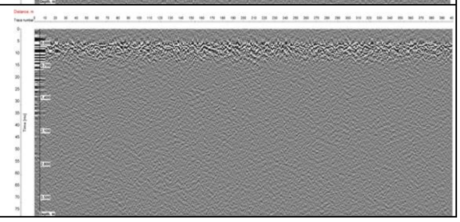 |

The results showed that sticlotextolite that makes up the stabilized system, part of which passed under the GPR antenna to provide increased stability, did not influence the measurements in any way, its presence being indicated in neither of the two measurements. A second observation is that the engines put into operation did not cause interference.

The second scenario was reproduced in the laboratory and was performed after mounting the stabilized support containing the 800 MHz GPR antenna on the drone. The measurements were made using the same parameters, with the antenna in the same position and the motors of the drone powered by electricity (simulating a flight by turning them at different rotations per minute).

In the first measurement it is observed that there are numerous interferences produced by the operation of the drone engines. These interferences are of different amplitude, duration and frequency depending on how the motors were run. It has been observed that the interference intensity is directly proportional to the engine speed. To eliminate this problem, a glass-coated glass cover was created around the GPR antenna, covered on the inside with copper foil, acting partially as a Faraday cage. The role of the copper foil is to shield the electromagnetic field produced by the drone's motors, so that the acquired data will no longer be interfering. The second measurement was performed in the conditions in which the first one was performed, the only difference being the presence of the glass-textile protection, as can be seen in the recording, the interference produced by the motors is no longer noticeable. In addition, the built-in protection did not induce other data changes.

*Table 6*

**Check for interference caused by drone engines**

| | |
|---|---|
| Test with engines running | 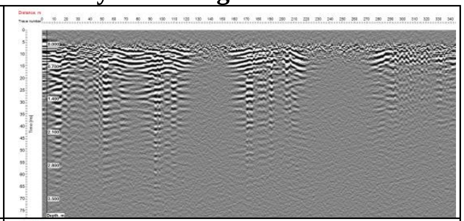 |
| Test with engines running and antenna protection | 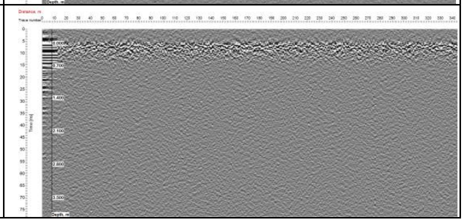 |

Fig. 5. Glass-textured protection covered inside with copper foil for GPR antenna

## 4. Conclusions

The purpose of this paper was to present the design and construction of a subset of real-time remote viewing and control for the existing GPR system, could perform GPR investigations from the air but also to ensure the quality of the acquired data. To mount the GPR system on the unmanned aerial system, a 3D gyro-stabilization system was designed and built with the role of stabilizing the antenna during data acquisition to minimize errors.

Laboratory tests have been performed to verify that the subassemblies created do not interfere with the data acquired by the GPR. The results obtained were encouraging for further research.

The use of such a system brings many benefits compared to the classic one used, from the ground, and allows the corroboration with other data obtained by aerial overflight, thus obtaining a complex package of information that offers the possibility to characterize not only the ground surface but also of the subsoil.

Carrying out aerial GPR investigations from low altitude brings many novelty elements and major advantages like the possibility to investigate difficult areas, higher investigation speed than ground coupled GPR, a larger area covered during measurements, etc. This paper's focus is on the novelty of upgrading an older GPR system to be able to perform investigation from low altitude, even though it doesn't have remote control and visualization features.

**Acknowledgment**

This paper is supported by a grant from the Romanian Ministry of Education and Research, CCCDI - UEFISCDI, project number PN-III-P2-2.1-PTE-2019-0492, within PNCDI III.

R E F E R E N C E S

[1] *A. Chelmus, R. Radvan and L. Angheluta*, "Aerial Investigations Corroboration for Archaeology and Monuments", 2018 11th International Conference on Developments in eSystems Engineering (DeSE), 2018, pp. 113-116.

[2] *Robert LK / David Hurst Thomas*, Archeology, Fifth edition, Cengage Learning, Belmont California, 2009.

[3] *KY. Kim, J.Lee, MH. Hong, JK. Hong, H. Shon*, "Helicopter borne and ground-towed radar survey of the Fourcade Glacier on King George Island, Antarctica", Exploration Geophysics 41 (1), 2010, pp. 51–60.

[4] *H. Machguth, O. Eisen, F. Paul, and M. Hoelzle*,"Strong spatial variability of accumulation observed with helicopter-borne GPR on two adjacent Alpine glaciers", Geophysical Research Letters 33 (13), 2006.

[5] *F. Soldovieri, I. Catapano, L. Crocco, G. Gennarelli, C. Papa*, "Low-frequency SOUNDER radar system as a new tool for archaeological prospection and monitoring: potentialities and preliminary surveys", 4th EARSeL Workshop on Cultural and Natural Heritage Proceedings, Matera, 2013.

[6] *F. Soldovieri*, "Applications of GPR and other non-destructive testing methods in archaeological prospecting and cultural heritage diagnostics", TUD COST Action TU1208 Civil Engineering Applications of Ground Penetrating Radar, Proceedings First Action's General Meeting, 2013

[7] *D. Ene, R. Radvan*, "Comparison of radar exploration from ground and low altitude for fast archaeological dissemination", Optoelectronics and Advanced Materials-Rapid Communications 5, 7, 2011, pp. 806–808.

[8] *S. Davarzani, I. Pisica, L. Lipan*, "Novel model for defining electricity tariffs using residential load profile characterization", International Journal of Renewable Energy Technology, International Journal of Renewable Energy Technology 9 (4): 383, January 2018.

[9] *C. Chousidis, R. Nilavalan, L. Lipan*, "Expanding the use of CTS-to-Self mechanism for reliable broadcasting on IEEE 802.11 networks," Wireless Communications and Mobile Computing Conference (IWCMC), 2014 International, 4-8 Aug. 2014, Pp.1051-1056.

[10] *G.C. Lazaroiu, L. Roscia et al*., "Influence of voltage flicker propagation on power systems operation", IEEE Conference: General Meeting of the IEEE Power-and-Energy-Society (PES), art. no. 6039773, Location: Detroit, 2011, pp. 1-6,

[11] *G.C. Lazaroiu, M. Roscia*, "Definition methodology for the smart cities model", Energy Journal, Volume 47, Issue 1, 2012, pp. 326-332.